THE JOURNAL OF BIOLOGICAL CHEMISTRY VOL. 280, NO. 48, pp. 40375–40383, December 2, 2005

Characterization of Archaeal Group II Chaperonin-ADP-Metal Fluoride Complexes

IMPLICATIONS THAT GROUP II CHAPERONINS OPERATE AS A "TWO-STROKE ENGINE"[*][S]

Received for publication, June 22, 2005, and in revised form, September 8, 2005 Published, JBC Papers in Press, September 23, 2005, DOI 10.1074/jbc.M506785200

Ryo Iizuka[‡], Takao Yoshida[‡§], Noriyuki Ishii[¶], Tamotsu Zako[‡‖], Kazunobu Takahashi[**], Kosuke Maki[**], Tomonao Inobe[**], Kunihiro Kuwajima[**], and Masafumi Yohda[‡1]

*From the [‡]Department of Biotechnology and Life Science, Tokyo University of Agriculture and Technology, 2-24-16 Naka-cho, Koganei, Tokyo 184-8588, [§]Research Program for Marine Biology and Ecology, Extremobiosphere Research Center, Japan Agency for Marine-Earth Science and Technology, 2-15 Natsushima-cho, Yokosuka, Kanagawa 237-0061, [¶]Biological Information Research Center, National Institute of Advanced Industrial Science and Technology, Tsukuba Central-6, 1-1-1 Higashi, Tsukuba, Ibaraki 305-8566, [‖]Bioengineering Laboratory, RIKEN, 2-1 Hirosawa, Wako, Saitama 351-0198, and the **Department of Physics, Graduate School of Science, The University of Tokyo, 7-3-1 Hongo, Bunkyo-ku, Tokyo 113-0033, Japan*

Group II chaperonins, found in Archaea and in the eukaryotic cytosol, act independently of a cofactor corresponding to GroES of group I chaperonins. Instead, the helical protrusion at the tip of the apical domain forms a built-in lid of the central cavity. Although many studies on the lid's conformation have been carried out, the conformation in each step of the ATPase cycle remains obscure. To clarify this issue, we examined the effects of ADP-aluminum fluoride (AlF_x) and ADP-beryllium fluoride (BeF_x) complexes on α-chaperonin from the hyperthermophilic archaeum, *Thermococcus* sp. strain KS-1. Biochemical assays, electron microscopic observations, and small angle x-ray scattering measurements demonstrate that α-chaperonin incubated with ADP and BeF_x exists in an asymmetric conformation; one ring is open, and the other is closed. The result indicates that α-chaperonin also shares the inherent functional asymmetry of bacterial and eukaryotic cytosolic chaperonins. Most interestingly, addition of ADP and BeF_x induced α-chaperonin to encapsulate unfolded proteins in the closed ring but did not trigger their folding. Moreover, α-chaperonin incubated with ATP and AlF_x or BeF_x adopted a symmetric closed conformation, and its functional turnover was inhibited. These forms are supposed to be intermediates during the reaction cycle of group II chaperonins.

Chaperonins, one of the most well studied molecular chaperones, are ubiquitous and indispensable proteins that are involved in protein folding in the cell. They assist in protein folding reactions both *in vivo* and *in vitro* by binding unfolded proteins within the central cavity of the double ring structure (1, 2). Based on protein sequence and structural features, chaperonins fall into two groups (2, 3). Group I chaperonins are found in bacteria, endosymbiotic organelles (mitochondria and chloroplasts), and only subsets of Archaea (4, 5). The most extensively characterized member is the *Escherichia coli* chaperonin GroEL and its partner GroES. GroEL-mediated protein folding requires GroES as a lid of the GroEL cavity. GroEL is functionally asymmetrical and is referred to as a "two-stroke engine," with one ring binding ATP and GroES, and simultaneously acting as the place where protein folding occurs, followed by an identical reaction on the opposite ring (6–8). In contrast, group II chaperonins, found in Archaea (called thermosome) and the eukaryotic cytosol (known as CCT or TCP-1 ring complex), work without the cofactor corresponding to GroES. The helical protrusion at the tip of the apical domain substitutes for the cofactor as a built-in lid of the central cavity. Many studies on the change of the lid's conformation coupled to the binding and hydrolysis of nucleotides have been carried out. It was found that ATP drives the conformational change of group II chaperonins from the open lid, substrate binding conformation to the closed lid conformation to encapsulate unfolded protein in the central cavity (9–15). However, the details of the ATP-driven reaction in group II chaperonins remain obscure. Meyer *et al.* (13) suggested that lid closure of CCT is induced not by the binding but by the hydrolysis of ATP. In contrast, similar experiments on archaeal chaperonins have shown that the trigger of lid closure is ATP binding (10, 14, 15). It is also curious that little asymmetry in the reaction cycle has been reported for group II chaperonins (13, 16).

To address these issues, we conducted a structural and functional characterization of ADP-metal fluoride complexes of α-chaperonin from the hyperthermophilic archaeum, *Thermococcus* sp. strain KS-1 (*T.* KS-1)[2] (17, 18). Metal fluorides, particularly aluminum fluoride (AlF_x) and beryllium fluoride (BeF_x), are widely utilized to analyze the functional cycle of numerous NTPases (*e.g.* Refs. 19–21). They have also been used to study the functional cycle of chaperonins (9, 13, 22–26). The crystal structure of the *Thermoplasma* chaperonin complexed with ADP and AlF_x (Protein Data Bank code 1A6E) provided the enzymatic information on the mechanism of ATP hydrolysis (9). Also, addition of ADP and metal fluorides to CCT induces the transition from a high affinity state for substrates to a low affinity state (13, 22). Moreover, Meyer *et al.* (13) reported that when incubated with ADP and AlF_x, CCT

* This work was supported in part by Grants-in-aid for Scientific Research on Priority Areas 15032212 and 17028013 and a grant from the National Project on Protein Structural and Functional Analyses from the Ministry of Education, Science, Sports, and Culture of Japan (to M. Y.). This work is part of the 21st Century Center of Excellence program of "Future Nano-Materials" research and education project supported by the Ministry of Education, Science, Sports, Culture, and Technology through Tokyo University of Agriculture & Technology. The SAXS experiments were performed with the approval of the Photon Factory (Proposal 2004G385). The costs of publication of this article were defrayed in part by the payment of page charges. This article must therefore be hereby marked "*advertisement*" in accordance with 18 U.S.C. Section 1734 solely to indicate this fact.

[S] The on-line version of this article (available at http://www.jbc.org) contains Figs. S1 and S2.

[1] To whom correspondence should be addressed: Dept. of Biotechnology and Life Science, Tokyo University of Agriculture and Technology, 2-24-16 Naka-cho, Koganei, Tokyo, 184-8588, Japan. Tel./Fax: 81-42-388-7479; E-mail: yohda@cc.tuat.ac.jp.

[2] The abbreviations used are: *T.* KS-1, hyperthermophilic archaeum *Thermococcus* sp. strain KS-1; CCT, chaperonin-containing *t*-complex polypeptide-1; αWT, *T.* KS-1 wild-type α-chaperonin; αL265W, L265W mutant of *T.* KS-1 α-chaperonin; AlF_x, aluminum fluoride; BeF_x, beryllium fluoride; SAXS, small-angle X-ray scattering; CS, citrate synthase; Cy5-CS, citrate synthase labeled with Cy5; GFP, green fluorescent protein; AMP-PNP, adenosine 5′-(β,γ-imino)triphosphate.

Supplemental Material can be found at: http://www.jbc.org/cgi/content/full/M506785200/DC1

has an asymmetric structure; one of the rings is open, and the other is closed. Here we found that *T.* KS-1 α-chaperonin incubated with ADP and BeF_x has an asymmetric structure, whereas that incubated with ATP and AlF_x or BeF_x has a symmetric closed conformation. These forms are considered to be intermediates in the functional cycle of group II chaperonins. The implications for the cycle are discussed.

EXPERIMENTAL PROCEDURES

Proteins and Reagents—*T.* KS-1 α-chaperonins were expressed in *E. coli* cells and purified as described previously (14). The concentrations of α-chaperonins were determined with the Bio-Rad protein assay, using bovine serum albumin as the standard, and were expressed as molar concentrations of hexadecamer in this paper. Citrate synthase (CS) from porcine heart was obtained from Sigma. The ammonium sulfate suspension of CS was desalted on a NAP-5 column (Amersham Biosciences) before use. The monomeric concentration of CS was determined spectrophotometrically at 280 nm with an extinction coefficient of 65,900 M^{-1} cm^{-1}. The GFP employed in this study is a thermostable mutant to perform assays at 60 °C (12, 27). It was expressed and purified as described (28). The concentration of GFP was determined spectrophotometrically at 280 nm with an extinction coefficient of 18,850 M^{-1} cm^{-1}. Proteinase K was from Ambion Inc. (Austin, TX). Nucleotides, NaF, $Al(NO_3)_3$, and $BeSO_4$ were purchased from Wako Pure Chemical Industries, Ltd. (Osaka, Japan). ADP was treated with hexokinase (Roche Diagnostics) plus glucose to remove contaminating ATP before use as described (29).

Generation of Chaperonin-ADP-Metal Fluoride Complexes—α-Chaperonin-ADP-metal fluoride complexes were prepared by the incubation of 1 mM ATP/ADP, 30 mM NaF, and 5 mM $Al(NO_3)_3$/$BeSO_4$ for 60 min at 60 °C in HKM buffer (20 mM HEPES-NaOH, pH 7.5, 100 mM KCl, and 5 mM $MgCl_2$), with exceptions specially described. The presence of sulfate ion (5 mM) did not affect the conformation of the chaperonins (data not shown).

Quantitation of Bound Nucleotide—αWT (1 μM) was incubated with nucleotides (1 mM) in the absence and presence of metal fluoride for 60 min at 60 °C, and the mixtures were applied to a NAP-5 column equilibrated with HKM buffer to remove unbound nucleotides. Isolated αWT-nucleotide complexes were treated with ice-cold perchloric acid at a final concentration of 2.5% and then were centrifuged. Aliquots of the supernatant were analyzed by a reverse-phase column (TSKgel ODS-80Ts, Tosoh, Japan) with 30 mM sodium phosphate buffer, pH 6.8, containing 2% (v/v) methanol at the flow rate of 0.5 ml/min using an Alliance HPLC System (Waters, Milford, MA). The eluate was monitored with an on-line UV spectrophotometer (Waters 996 photodiode array detector) at 259 nm, and the amount of nucleotide was calculated using peak area.

Protease Sensitivity Assay—αWT (100 nM) was incubated with or without nucleotide (1 mM) and metal fluorides at 60 °C in HKM buffer under continuous mixing. Digestion with proteinase K (0.25 ng/μl) was carried out for 5 min at 60 °C. Proteins in the reaction mixture were precipitated by the addition of trichloroacetic acid and then analyzed on 15% SDS gels. Gels were stained with Coomassie Brilliant Blue R-250. Band intensities were quantitated using Scion Image software (Scion Corp., Fredrick, MD).

Fluorescence Measurements—The tryptophan fluorescence spectra of αL265W (14) were measured at 60 °C with a Jasco FP-6500 spectrofluorometer (Jasco, Tokyo, Japan). The excitation wavelength was set at 295 nm, and the emission was recorded from 310 to 450 nm (bandwidth = 3 nm for excitation and 5 nm for emission). αL265W (0.2 μM) was preincubated with or without nucleotide (1 mM) and metal fluorides at 60 °C, and the mixture was stirred throughout the measurement. Fluorescence intensity (I) was calculated from $I_{corrected} = I_{sample} - I_{blank}$ where the blank contained all other components of the assay mixture except αL265W. All spectra obtained were the average of five scans.

Electron Microscopy and Image Processing—αWT (100 nM) was incubated with nucleotides (1 mM) and BeF_x at 60 °C, and the aliquots were negatively stained in 1% uranyl acetate for 30 s on thin carbon support film, which was hydrophilized by a hydrophilic treatment device (JEOL Datum HDT-400). The specimen grids were scanned at low magnification under dark illumination to reduce radiation damage. After adjusting the astigmatism and focus at adjacent areas, images of target area were recorded by making use of a slow scan CCD camera (Gatan Retractable Multiscan Camera) under low electron dose conditions at a magnification of ×50,000 in a Philips Tecnai F20 electron microscope operated at 120 kV. The images were processed with a digital micrograph (Gatan Inc.) followed by the SPIDER image processing system (Health Research Inc., New York) for single particle analysis (30). For each data set with the desired experimental condition, appropriate images of monodispersed particles were selected and rotated to maximize correlation. Normalized cross-correlation function between any two pictures was calculated successively by using Fourier transform relationship. Finally, the pictures derived from the monodispersed particles were averaged after rejecting the particles that correlated poorly by using SPIDER/WEB system on an SGI UNIX cluster (31).

SAXS Measurements—The SAXS experiments were performed with beamline 15A at the Photon Factory of the High Energy Accelerator Research Organization, Tsukuba, Japan. The measurements were made with protein concentrations of 7 mg/ml in HKM buffer at 60 °C. Before data collection, the protein solutions were incubated with or without nucleotides (1 mM) and BeF_x at 60 °C. Scattering patterns were recorded by a CCD-based x-ray detector, which consisted of a beryllium-windowed x-ray image intensifier (Be-XRII) (Hamamatsu, V5445P-MOD), an optical lens, a CCD image sensor, and a data acquisition system (Hamamatsu C7300), as described (32, 33). The experimental details and the analyses of the scattering data were described in Ref. 32. Pair distribution ($P(r)$) functions were calculated by using the GNOM program (34). The Q range used for the calculation was from 0.0156 to 0.170 $Å^{-1}$. The values of radius of gyration (R_g) and maximum particle distance (D_{max}) were derived from the $P(r)$ function.

Thermal Aggregation Measurements—The thermal aggregation of CS was monitored by measuring light scattering at 500 nm with a spectrofluorometer (FP-6500) for 30 min at 50 °C. Native CS was diluted to a final concentration of 100 nM (as a monomer) in HKM buffer with or without αWT (50 nM). The reaction mixtures were preincubated for 10 min at 50 °C and continuously stirred throughout the measurement.

GFP Refolding Assays—GFP (5 μM) was denatured in the folding buffer (20 mM Tris-HCl, pH 7.5, 100 mM KCl, 5 mM $MgCl_2$, and 5 mM dithiothreitol) containing 100 mM HCl at room temperature, and diluted 100-fold in the folding buffer with or without αWT (100 nM). αWT was complexed with ADP and BeF_x by incubation with 1 mM ADP, 30 mM NaF, and 5 mM $BeSO_4$ for 60 min at 60 °C in the folding buffer. Nucleotides were added to a final concentration of 1 mM in the mixture 5 min after the dilution of denatured GFP. The fluorescence of GFP at 510 nm with excitation at 396 nm was continuously monitored for 30 min with a Jasco FP-6500 spectrofluorometer. The reaction mixtures were continuously stirred at 60 °C throughout the assays. As a control, native GFP was diluted in the folding buffer without αWT. The fluorescence intensity of native GFP was taken as 100%.

TABLE ONE

Amounts of nucleotides bound to αWT in the absence and presence of metal fluorides

Row	Complex was formed in	Nucleotide species	Nucleotide/αWT[a]
			mol/mol
1	ATP	ATP	0.76 ± 0.04
		ADP	0.72 ± 0.03
2	ADP	ADP	1.3 ± 0.3
3	ATP+AlF_x	ATP	2.1 ± 0.9
		ADP	6.2 ± 0.6
4	ADP+AlF_x	ADP	4.8 ± 2.4
5	ATP+BeF_x	ATP	2.0 ± 1.1
		ADP	5.2 ± 0.4
6	ADP+BeF_x	ADP	5.3 ± 0.8

[a] Data represent mean ± S.D. (n = 3).

Preparation of Cy5-CS and the Amount of Cy5-CS in the Chaperonin Cavity—Before labeling, CS was desalted on a NAP-5 column equilibrated with 50 mM sodium phosphate, pH 7.5. After mixing of 200 μl of CS (22.4 μM, as a monomer) with 20 μl of 1 M Na_2HPO_4, Cy5 monoreactive dye (Amersham Biosciences) was added to 83 μM, and the mixture was incubated for 3 h at room temperature. The unreacted Cy5 was then removed with a NAP-5 column. The extent of the labeling was determined by absorption spectroscopy. The molar ratio of Cy5 to CS monomer was 1.4. The fluorescent-labeled CS is designated Cy5-CS.

Cy5-CS (100 nM, as a monomeric concentration) was diluted in HKM buffer containing 50 nM αWT, 30 mM NaF, and 5 mM $BeSO_4$. Nucleotides (1 mM) were added to the mixture 5 min after the dilution. After incubation for 60 min at 60 °C, proteinase K (0.25 ng/μl) was added. After a 30-min digestion at 60 °C, phenylmethanesulfonyl fluoride was added at a final concentration of 2 mM, and the aggregated Cy5-CS was removed by centrifugation (17,000 × *g*, 10 min, 4 °C). The supernatant was precipitated using trichloroacetic acid and then applied to a 10% SDS gel. The gel was visualized using Coomassie Brilliant Blue R-250 and an image analyzer, Typhoon 8600 (Amersham Biosciences), with excitation at 633 nm and a 670 BP 30 (Cy5) emission filter.

RESULTS

Preparation of Chaperonin-ADP-Metal Fluoride Complexes—We employed aluminum fluoride and beryllium fluoride (termed AlF_x and BeF_x) to elucidate details of the group II chaperonin reaction cycle. AlF_x and BeF_x act as structural analogs of inorganic phosphate and have been used to study a variety of NTPases (*e.g.* Refs. 19–21). They are bound to the nucleotide-binding pockets with ADP, and the complexes are interpreted as mimicking the ground state (BeF_x) and the transition state (AlF_x) of NTP hydrolysis and block further nucleotide exchange (19, 20). In this study, *T.* KS-1 α-chaperonin-ADP-metal fluoride complexes were prepared in the following two ways: (i) mixing α-chaperonin with ADP and metal fluoride (referred to as ADP + AlF_x and ADP + BeF_x), and (ii) substituting metal fluoride for inorganic phosphate generated by ATP hydrolysis of α-chaperonin (referred to as ATP + AlF_x and ATP + BeF_x).

At the beginning of this study, the amounts of nucleotides bound to wild-type α-chaperonin (αWT) were examined (TABLE ONE). Total nucleotide-binding sites of *T.* KS-1 α-chaperonin complex are estimated to be 16 (8 binding sites per ring). Neither ATP nor ADP was found in the purified proteins (data not shown). αWT in the absence of metal fluoride did not bind nucleotides tightly, and small amounts of bound nucleotides were detected (TABLE ONE, rows 1 and 2). On the other hand, αWT in the presence of metal fluorides formed relatively stable complexes with ADP and contained 5–6 mol of ADP per mol (TABLE ONE, rows 3–6). AlF_x and BeF_x should take the place of the γ-phosphate of ATP and stabilize the association of αWT with ADP. In the presence of ATP, both ATP and ADP were bound to αWT (TABLE ONE, rows 1, 3, and 5), suggesting that one ring may be saturated with metal fluoride and ADP generated by the hydrolysis of ATP, and ATP remains in the other ring. Although there are 16 nucleotide-binding sites in αWT, only about 8 nucleotides were observed in the present study. This is probably because of the relatively low affinity of nucleotides to αWT as shown in the results of the experiments without metal fluorides. Several nucleotides should be lost during gel filtration by the NAP-5 column. It is also reported that GroEL is unable to bind nucleotides tightly in the absence of GroES (35, 36).

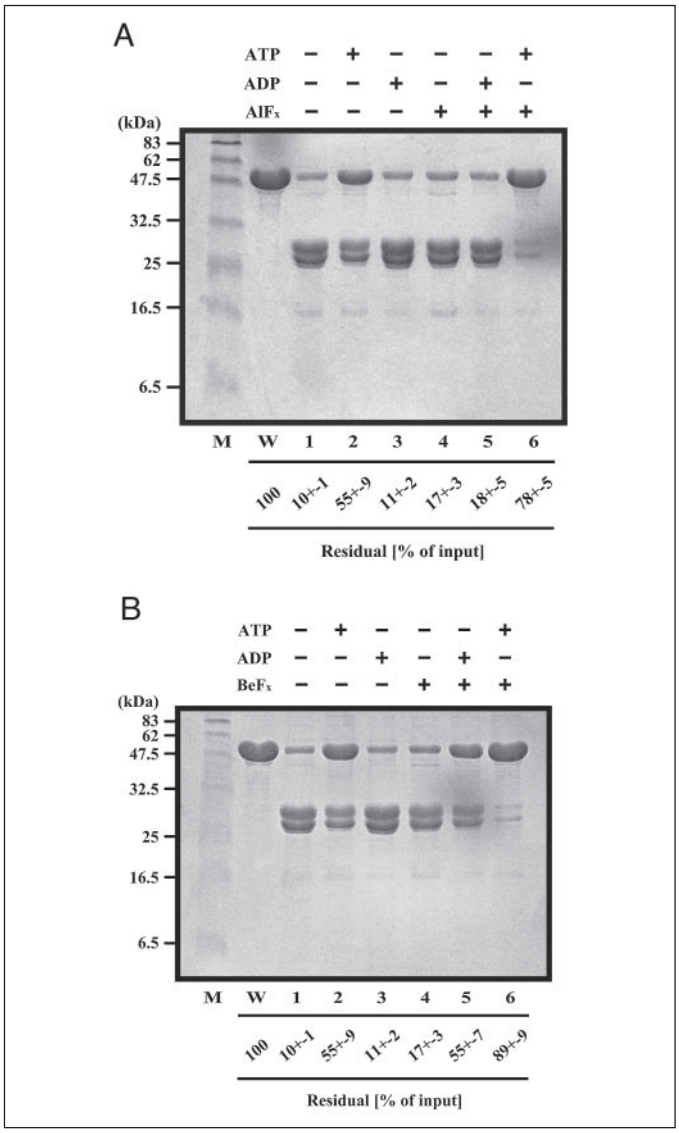

FIGURE 1. **Protease sensitivity assay of αWT in the absence and presence of metal fluorides.** αWT incubated with or without nucleotide (1 mM) and metal fluorides (*A*, AlF_x; *B*, BeF_x) was exposed to proteinase K (0.25 ng/μl) and then analyzed by SDS-PAGE. The experimental details are described under "Experimental Procedures." *Lane M*, molecular weight marker; *lane W*, αWT; *lane 1*, without addition of nucleotide; *lane 2*, incubated with ATP; *lane 3*, incubated with ADP; *lane 4*, incubated with metal fluoride; *lane 5*, incubated with ADP + metal fluoride; *lane 6*, incubated with ATP + metal fluoride. Band intensities were quantified and analyzed using Scion Image software. The *error bar* is the standard deviation of three different assays.

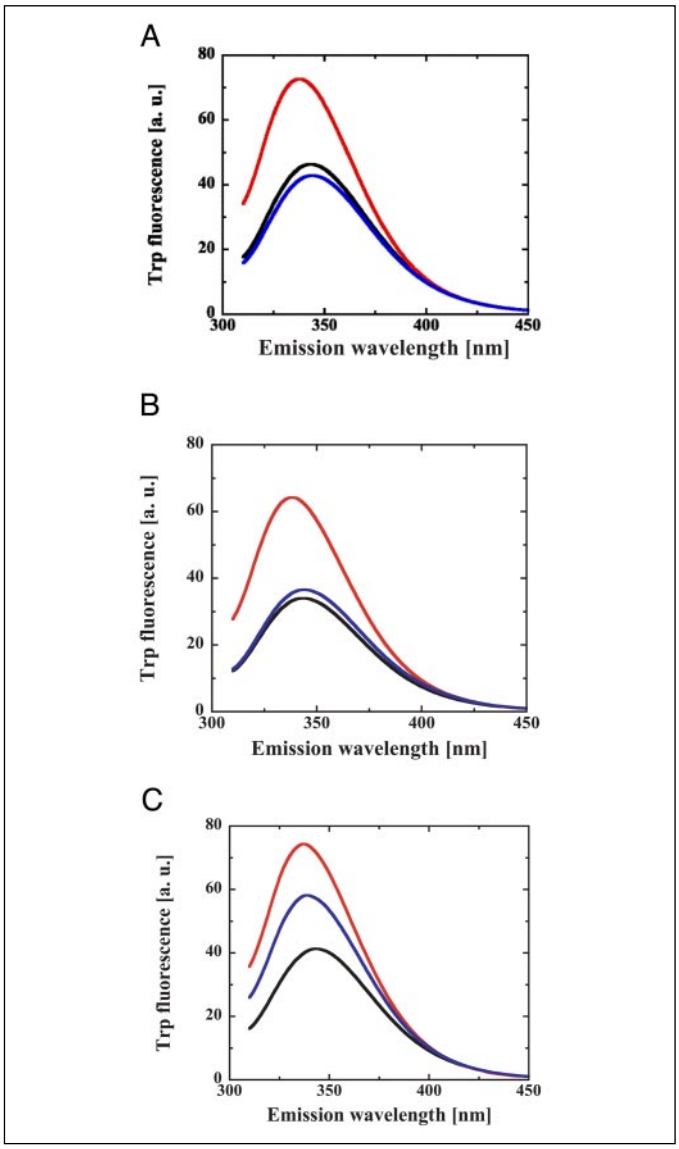

FIGURE 2. **Fluorescence spectra of αL265W in the absence and presence of metal fluorides.** Tryptophan fluorescence spectra of αL265W were obtained in the absence (*A*) and presence of metal fluorides (*B*, AlF_x; *C*, BeF_x). The experimental details are described under "Experimental Procedures." *Black line*, without addition of nucleotides; *red line*, incubated with ATP; *blue line*, incubated with ADP. *a.u.*, arbitrary units.

It is expected that there are conformational differences between α-chaperonin incubated with ADP + metal fluoride and with ATP + metal fluoride. Subsequently, structural and functional analyses were performed.

Conformation of the Lids of Chaperonin-ADP-Metal Fluoride Complexes—Initially, protease sensitivity assays of αWT with or without nucleotides and metal fluorides were conducted using proteinase K (Fig. 1). Previously, we revealed that the pattern of digestion of αWT by proteases differs according to the lid's conformation; the open lid conformation (nucleotide-free or ADP-bound form) is susceptible to proteases, and the closed lid conformation (ATP-bound form) is resistant (14, 15). In the presence of ATP, αWT was relatively proteinase K-resistant and polypeptides of about 60 kDa, corresponding to the undigested αWT, remained (Fig. 1, *lane 2*). In contrast, the 60-kDa polypeptides almost completely disappeared in the absence of nucleotide or the presence of ADP (Fig. 1, *lanes 1* and *3*). αWT incubated with ADP + AlF_x did not show protease resistance (Fig. 1*A*, *lane 5*). The result was the same irrespective of the aluminum salt species ($AlCl_3$ and $AlK(SO_4)_2$) (data not shown). On the other hand, incubation with ADP + BeF_x caused a half-level of protection (Fig. 1*B*, *lane 5*). It has been demonstrated previously that CCT is more resistant to proteinase K at the helical protrusion in the presence of ADP + AlF_x than in the presence of ADP + BeF_x or the absence of nucleotide (13). Our results were the opposite of those obtained previously with CCT. Besides, the incubation with ATP + AlF_x or BeF_x provided a substantial level of protection (Fig. 1, *lane 6*).

Additionally, we examined the lid's conformations by analyzing the fluorescence spectra of the tryptophan at the tip of the helical protrusion of a mutant, αL265W (14). Addition of ATP to αL265W caused a large increase (about 60%) in tryptophan fluorescence intensity, with a detectable blue shift in the wavelength of the emission maximum (Fig. 2*A*, *red line*, and TABLE TWO). On the other hand, a slight decrease in fluorescence was observed on the addition of ADP (Fig. 2*A*, *blue line*, and TABLE TWO). An increase in fluorescence was induced by incubation with ADP + BeF_x (about 41%) with a slight blue shift in the emission maximum, whereas a tiny increase (about 7.6%) was observed on incubation with ADP + AlF_x (Fig. 2, *B* and *C*, *blue line*, and TABLE TWO). Also, αL265W incubated with ATP + metal fluorides indicated both a blue shift and a marked enhancement of fluorescence emission (AlF_x, about 89%; BeF_x, about 80%) (Fig. 2, *B* and *C*, *red line*, and TABLE TWO). This series of results is in good agreement with the results of protease sensitivity assays (Fig. 1).

Structural Analyses of Chaperonin-ADP-Beryllium Fluoride Complexes—The above experiments (Figs. 1 and 2) have suggested that α-chaperonin adopts three different conformations in the presence of BeF_x according to added nucleotides. Next, we focused on the effect of BeF_x, and we compared the chaperonin conformations based on electron microscopy (Fig. 3) and small angle x-ray scattering (SAXS) measurements (Fig. 4 and TABLE THREE).

Fig. 3 shows the electron micrographs of αWT incubated with ADP + BeF_x and ATP + BeF_x. Without nucleotide, two typical shapes were observed; the more common top view and the less frequent side view (data not shown). After the incubation with ADP + BeF_x, side views of bullet-shaped particles were observed, which were similar to the GroEL and GroES complex (37) (Fig. 3*A*). For αWT incubated with ATP + BeF_x, mostly side views were obtained (Fig. 3*B*). Most particles adopted a football-like symmetric conformation, indicating that both rings were closed as observed in the crystal structures (9, 38). The closed ring structure of αWT incubated with ADP and BeF_x is almost indistinguishable from those of αWT incubated with ATP and BeF_x at the resolution level of the electron microscopic observation (supplemental Fig. S1). The symmetric conformation was also observed in αWT incubated with ATP + AlF_x (data not shown). Similar particles were reported previously in CCT incubated with ATP (39), with AMP-PNP (11), and with ATP + AlF_x (23).

We also applied SAXS to investigate the chaperonin conformations in the absence and presence of nucleotides (1 mM) and BeF_x (Fig. 4*A*). The scattering curves were interpreted in terms of the pair distribution ($P(r)$) function, which provide information about the distribution of the size and shape of the scattering particles (Fig. 4*B*). The $P(r)$ profiles of αWT under three different conditions (nucleotide-free, ATP + BeF_x, and ADP + BeF_x) were almost identical to those of nucleotide-free CCT, CCT complexed with ATP, and CCT complexed with ADP + AlF_x, respectively (13). The structural parameters obtained in this study are summarized in TABLE THREE. The values for the R_g and the D_{max} were derived from the $P(r)$ function using the program GNOM (34). As noted in previous studies (10, 13, 15), the nucleotide-free form and

TABLE TWO

Fluorescence parameters of αL265W

	Maximum of Trp fluorescence	Fluorescence at emission maximum	Relative fluorescence[a]
	nm	*arbitrary units*	
In the absence of metal fluoride			
Nucleotide-free	343	46.3	100
+ ATP	338	72.7	157
+ ADP	344	42.9	92.7
In the presence of AlF_x			
Nucleotide-free	344	34.0	100
+ ATP	338	64.2	189
+ ADP	344	36.6	108
In the presence of BeF_x			
Nucleotide-free	343	41.3	100
+ ATP	337	74.3	180
+ ADP	339	58.2	141

[a] Relative fluorescence intensity at emission maximum in the absence and presence of nucleotides. The intensity in the absence of nucleotide in each data set is taken as 100.

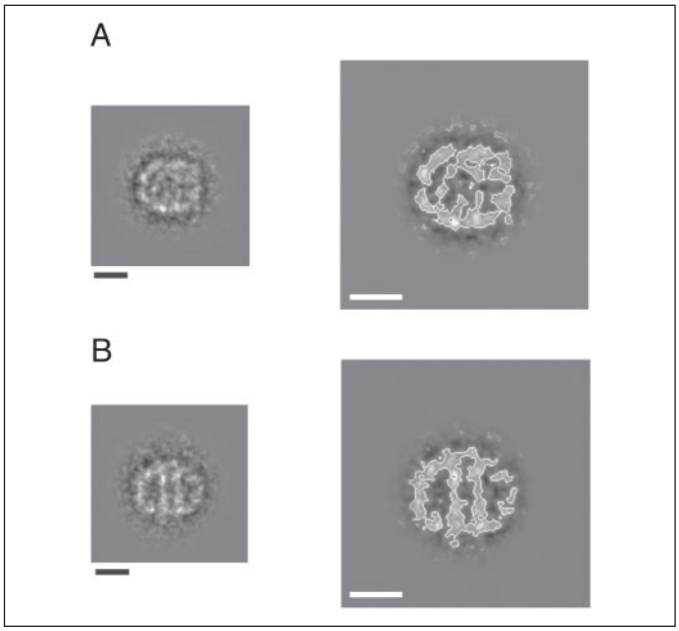

FIGURE 3. **Averaged side views of electron microscopic images of αWT incubated with ADP + BeF_x and with ATP + BeF_x.** αWT was incubated with ADP + BeF_x (*A*) and ATP + BeF_x (*B*) at 60 °C for 60 min and negatively stained with 1% uranyl acetate. *A*, averaged side view of αWT incubated with ADP + BeF_x ($n = 8$). *B*, averaged side view of αWT incubated with ATP + BeF_x ($n = 8$). The *right panels* show the enlarged ones with contour map. *Scale bar* represents 10 nm.

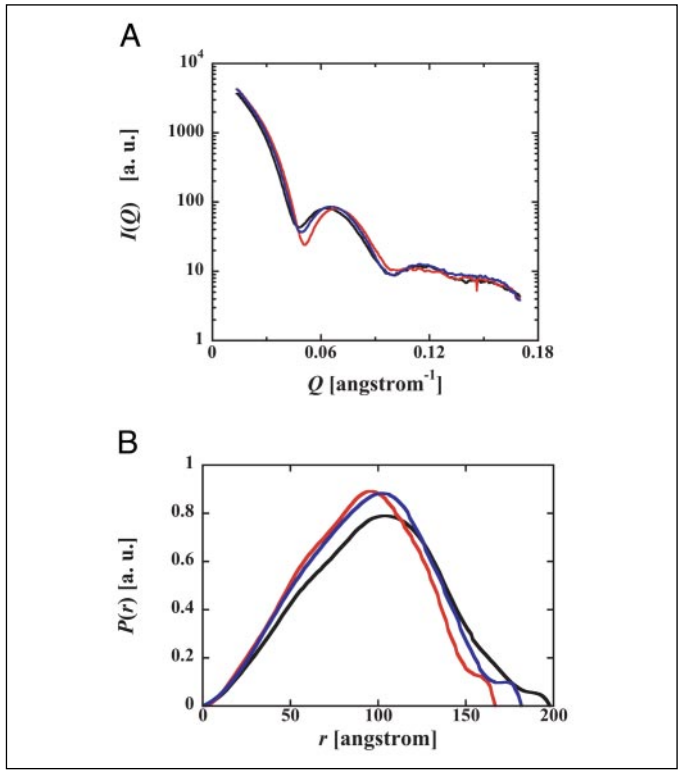

FIGURE 4. **SAXS analyses of αWT incubated without or with nucleotide and BeF_x.** *A*, scattering curves of αWT under three different sets of conditions. The scattering intensity $I(Q)$ is shown as a function of Q. Q is defined by $Q = 4\pi\sin\theta/\lambda$, where λ and 2θ are wavelength of x-ray and scattering angle, respectively. The experimental details are described under "Experimental Procedures." *Black line*, without addition of nucleotides; *red line*, incubated with ATP + BeF_x; *blue line*, incubated with ADP + BeF_x. *B*, pair distribution ($P(r)$) functions of αWT under three different sets of conditions. The functions were calculated using the GNOM program (33). *Black line*, without addition of nucleotides; *red line*, incubated with ATP + BeF_x; *blue line*, incubated with ADP + BeF_x.

ADP-bound form have an expanded conformation, exhibiting large values for R_g and D_{max}. These conformations are considered to be open lid conformations. On the other hand, ATP induces a significant conformational change in αWT, with a 1.8 Å decrease in R_g and a 13 Å diminution of D_{max}. The conformation in the presence of ATP + BeF_x is the most compact, with an R_g value of 67.0 Å and a D_{max} value of 167 Å. The calculated R_g and D_{max} values are in excellent agreement with the values predicted from the crystal structure of *Thermoplasma* chaperonin with the rings closed (9). In contrast, αWT incubated with ADP + BeF_x seems to take an intermediate shape between that in the absence and presence of ATP + BeF_x, *i.e.* an R_g value of 70.5 Å and a D_{max} value of 182 Å. The calculated R_g and D_{max} values are close to those of CCT incubated with ADP + AlF_x (13). The values are also in good agreement with those predicted from the hypothetical asymmetric structure, one open ring and one closed ring. Meyer *et al.* (13) reported that *ab initio* modeling for CCT complexed with ADP + AlF_x yielded an apparently asymmetric structure. Taken together with the biochemical assays (Figs. 1 and 2) and electron microscopic observations (Fig. 3), we have concluded that αWT complexed with ADP + BeF_x has an asymmetric conformation, one ring is open and the other is closed, whereas αWT complexed with ATP + BeF_x has a football-like conformation, and both rings are closed.

TABLE THREE

Structural parameters of group II chaperonins

Protein	Nucleotide	R_g	D_{max}
		Å	Å
Structural parameters of αWT[a]			
αWT	Free	74.1	197
	ATP	72.3	184
	ADP	74.9	201
	ADP+BeF_x	70.5	182
	ATP+BeF_x	67.0	167
Structural parameters of CCT[b]			
CCT	Free	70.2 ± 0.5	195 ± 5
	ATP	64.7 ± 0.6	171 ± 5
	ADP	69.4 ± 0.8	193 ± 3
	ADP+AlF_x	67.8 ± 0.9	182 ± 5
Structural parameters obtained by calculation[b]			
Open conformation		71.3 ± 0.6	203 ± 4
Asymmetric conformation		67.6 ± 0.7	179 ± 4
Closed conformation		64.8 ± 0.7	164 ± 5

[a] Data are from this work.
[b] Values were taken from Ref. 13.

Chaperone Function of Chaperonin-ADP-Beryllium Fluoride Complexes—Next, we investigated the chaperone function of the chaperonin complexed with ADP and BeF_x by using CS from porcine heart (Fig. 5). The extent of CS aggregation was monitored by light scattering. Native CS is a dimer of 48-kDa subunits that are prone to aggregate upon heat denaturation (Fig. 5*A*, *filled circles*). In the presence of αWT and ATP, the inhibitory effect decreased probably because of the ATP-dependent release of CS (Fig. 5*A*, *open circles*). Addition of ADP to the mixture of αWT slightly enhanced the inhibition of CS aggregation (Fig. 5*A*, *open squares*). αWT did not suppress CS aggregation at all in the presence of ATP + BeF_x (Fig. 5*B*, *open circles*), suggesting that it is unable to bind aggregation-prone intermediates of CS in a fully closed conformation. The effect of αWT incubated with ADP + BeF_x was almost the middle of those incubated with BeF_x and ATP + BeF_x (Fig. 5*B*, *open squares*). The result is additional proof for the asymmetric conformation of αWT complexed with ADP + BeF_x; one ring is in the closed conformation and the other is open for binding with an unfolded protein.

To investigate whether αWT is able to enhance folding of the substrate protein in the presence of BeF_x, GFP refolding assays were performed (Fig. 6*A*). Acid-denatured GFP was diluted into the assay mixtures containing αWT with or without BeF_x, and then nucleotides were added. The recovery of the native form was measured by its fluorescence in real time. In the presence of BeF_x, GFP fluorescence was recovered by αWT in an ATP-dependent manner (Fig. 6*A*, *open circles*), but the yield was lower than in the absence of BeF_x (*filled circles*). These results indicate that BeF_x inhibits the functional turnover of αWT. On the other hand, no recovery of GFP fluorescence was observed on the addition of ADP to αWT in the absence (Fig. 6*A*, *filled squares*) or presence of BeF_x (*open squares*). However, the addition of ATP to αWT incubated with ADP + BeF_x initiated GFP refolding despite the low yield (Fig. 6*A*, *open triangles*). Most interestingly, the folding yield was nearly half that in the presence of ATP + BeF_x (Fig. 6*A*, *open circles*). Moreover, αWT incubated with ATP + BeF_x did not inhibit the spontaneous refolding of GFP (data not shown). It is obvious that the substrate-binding site is shielded by the closed lid.

To assess the complex between αWT and the substrate in more detail, a protease sensitivity assay of the polypeptide bound to αWT was conducted (Fig. 6*B*). As the substrate, Cy5-labeled CS (termed Cy5-CS) was used. Cy5-CS was added to the chaperonin solutions containing BeF_x prior to the nucleotides and then exposed to proteinase K. The resultant solutions were applied to SDS-PAGE analysis. Little proteinase K-resistant Cy5-CS was observed without the addition of nucleotides (Fig. 6*B bottom panel*, *lane 1*). Polypeptides bound to αWT are

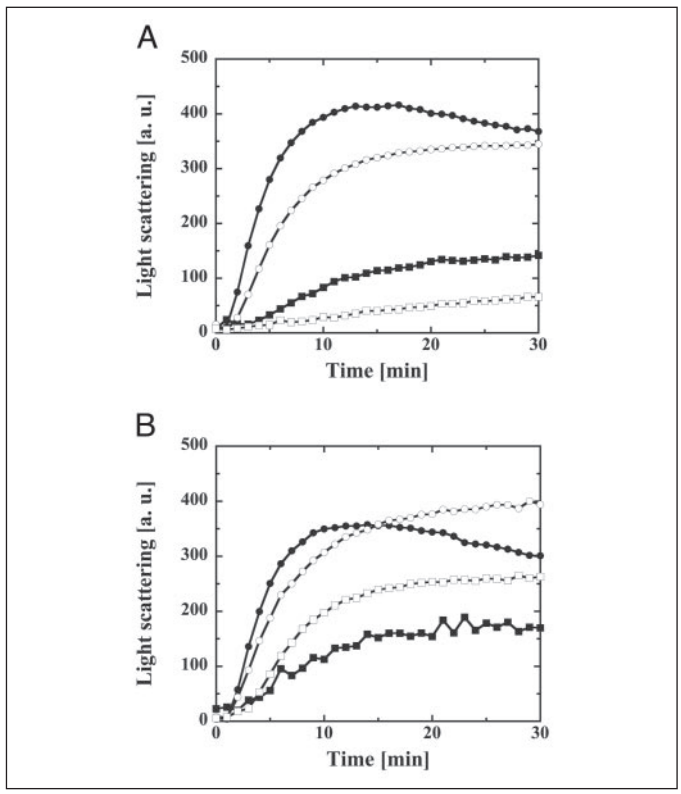

FIGURE 5. **Prevention of CS aggregation in the absence and presence of metal fluorides.** Effects of αWT incubated with nucleotides on the aggregation of CS at 50 °C were monitored in the absence (*A*) and presence of BeF_x (*B*). The experimental details are described under "Experimental Procedures." *Filled circles*, without αWT; *filled squares*, αWT without addition of nucleotides; *open circles*, αWT + ATP; *open squares*, αWT + ADP. *a.u.*, arbitrary units.

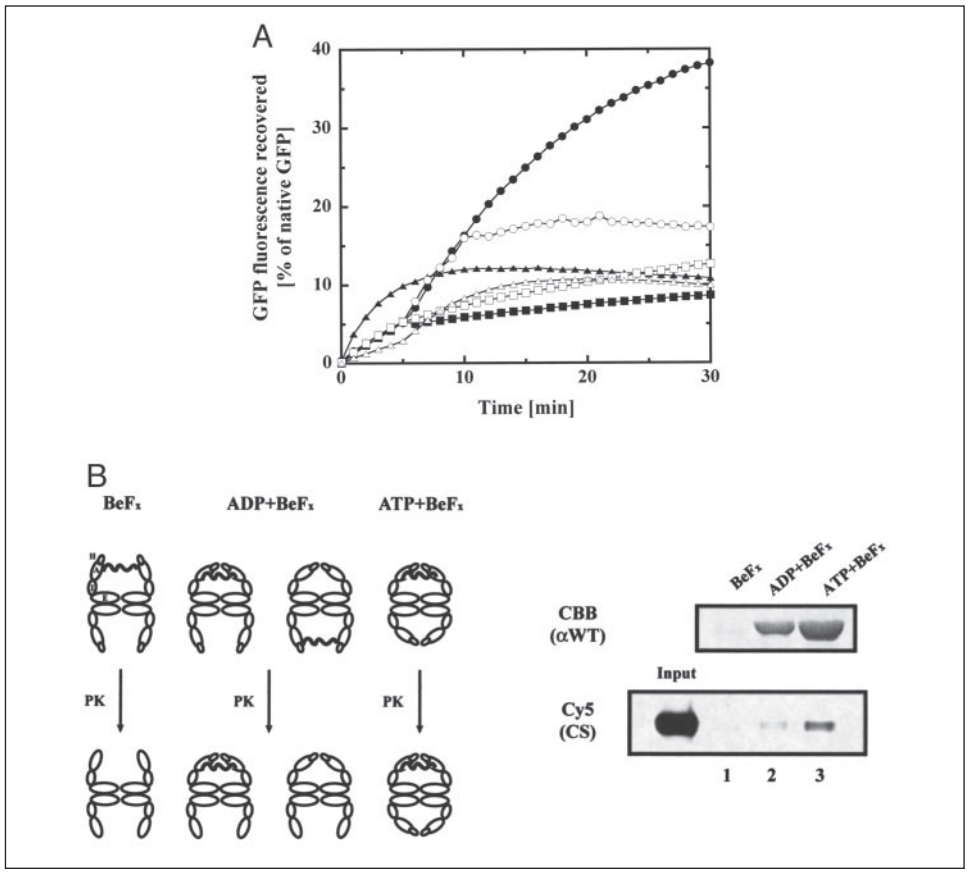

FIGURE 6. **αWT forms a stable complex with the substrate proteins in the presence of ADP and BeF_x.** *A,* αWT-mediated protein folding in the presence of BeF_x. The folding mixture was incubated at 60 °C as described under "Experimental Procedures." The recovery of GFP fluorescence was continuously monitored at 510 nm. The amount recovered is expressed as a percentage of the fluorescence intensity of native GFP. At 0 min, acid-denatured GFP (5 μM) was diluted 100-fold in the folding buffer containing 100 nM αWT and BeF_x. At 5 min after the dilution, 1 mM nucleotide was added. *Filled circles*, αWT + ATP; *filled squares*, αWT + ADP; *open circles*, αWT + ATP in the presence of BeF_x; *open squares*, αWT + ADP in the presence of BeF_x; *open triangles*, αWT incubated with ADP and BeF_x + ATP. Spontaneous refolding of GFP was observed upon dilution of denatured GFP in the folding buffer without αWT (*filled triangles*). *B,* protease sensitivity of αWT-Cy5-CS complexes. Cy5-CS was diluted in the mixtures with αWT and BeF_x before addition of nucleotides. The mixtures were subjected to digestion by proteinase K (*PK*) (0.25 ng/μl) for 30 min at 60 °C. Digestion was stopped by phenylmethylsulfonyl fluoride, and the mixtures were analyzed by SDS-PAGE. The gel was visualized using Coomassie Brilliant Blue (*CBB*) and a Typhoon 8600 image analyzer. *Left,* schematic drawing for the interpretation of the results. *A*, *I*, and *E* refer to the apical, intermediate, and equatorial domains, respectively. *H* represents the helical protrusion. *Right,* the relative amount of full-length αWT (*top panel*) and Cy5-CS (*bottom panel*). *Lane 1* without addition of nucleotide; *lane 2*, incubated with ADP + BeF_x; *lane 3*, incubated with ATP + BeF_x.

thought to be susceptible to proteolysis, although αWT is able to prevent CS thermal aggregation under nucleotide-free conditions (Fig. 5). Similar results were observed for GroEL (*e.g.* Ref. 40). By contrast, when ATP was added to the assay mixture, some Cy5-CS was protected from proteolysis (Fig. 6*B, bottom panel*, *lane 3*). In the presence of ADP + BeF_x, Cy5-CS also remained undigested (Fig. 6*B, bottom panel*, *lane 2*), even though one of the chaperonin rings had been exposed to proteinase K (*top panel*, *lane 2*). The time course data of Cy5-CS proteolysis is shown in supplemental Fig. S2. Cy5-CS was gradually digested by proteinase K, and almost all Cy5-CS was lost after 30 min of incubation in the absence of nucleotides. On the contrary, Cy5-CS was protected from the digestion in the presence of ADP and BeF_x. These observations suggested that Cy5-CS was encapsulated in the closed ring of αWT on the addition of ADP or ATP in the presence of BeF_x.

DISCUSSION

To grasp the details of an ATP-driven reaction cycle of the group II chaperonins, we characterized the structural and functional properties of *T.* KS-1 α-chaperonin in complexes with ADP and metal fluorides. The effects of AlF_x and BeF_x on the conformation of α-chaperonin were different when incubated with ADP. Biochemical (Figs. 1 and 2) and structural analyses (Figs. 3 and 4) revealed that α-chaperonin incubated with ADP + BeF_x has an asymmetric structure; one ring is open and the other ring is closed. It has been shown that CCT incubated with ADP + AlF_x adopted an asymmetric conformation, but BeF_x did not induce such a conformational change (13). Although our results partly contradict those reported in CCT, they strongly suggest that *T.* KS-1 α-chaperonin also shares the inherent functional asymmetry of GroEL (for reviews see Refs. 1 and 2) and CCT (13, 16).

We have shown previously that the change from an open lid to a closed lid conformation is not required for ATP hydrolysis in *T.* KS-1 α-chaperonin (14, 15). In the present study, we found that ADP + BeF_x, which is thought to mimic the ATP-bound state (19, 20, 24), induced the conformation on α-chaperonin with one ring closed. In contrast, it was shown that ADP + AlF_x, an analog of the trigonal-bipyramidal transition state in ATP hydrolysis, induced the lid closure of CCT (13). Therefore, reaction cycles of archaeal chaperonins and CCT are partly different from each other even though they are grouped together. ATP binding is sufficient to close the lid of archaeal chaperonins, whereas the lid closure of CCT is triggered by the transition state of ATP hydrolysis. Progress to the transition state mimicked by ADP + AlF_x might induce the opening of the lid in *T.* KS-1 α-chaperonin.

In GroEL, it is suggested that the binding of ATP is sufficient to encapsulate the substrate in the closed cavity. In addition, ATP hydrolysis is not required for protein folding mediated by GroEL (7, 25, 26). It is anticipated that the closure of the ring cavity leads to the folding of the substrate. Most unexpectedly, the addition of ADP to αWT in the presence of BeF_x did not support the folding of the unfolded protein encapsulated in the closed ring (Fig. 6). It appears that the substrate fails to be released into the central cavity, where productive folding occurs. Moreover, unfolded protein captured by αWT complexed with ADP + BeF_x can be folded by further incubation with ATP (Fig. 6*A*). Therefore, the conformation under ADP + BeF_x is considered to be the reaction intermediate in the functional cycle of group II chaperonins. This form is supposed to be able to encapsulate the protein in the closed ring without escaping into bulk solution. The presence of a similar intermediate in GroEL was pointed out previously (41, 42). In any case, it is thought that the ring is closed, and the substrate protein is encapsulated in the closed ring before the hydrolysis of ATP takes place. Most interestingly, only ATP can trigger productive protein folding inside the cavity. ATP

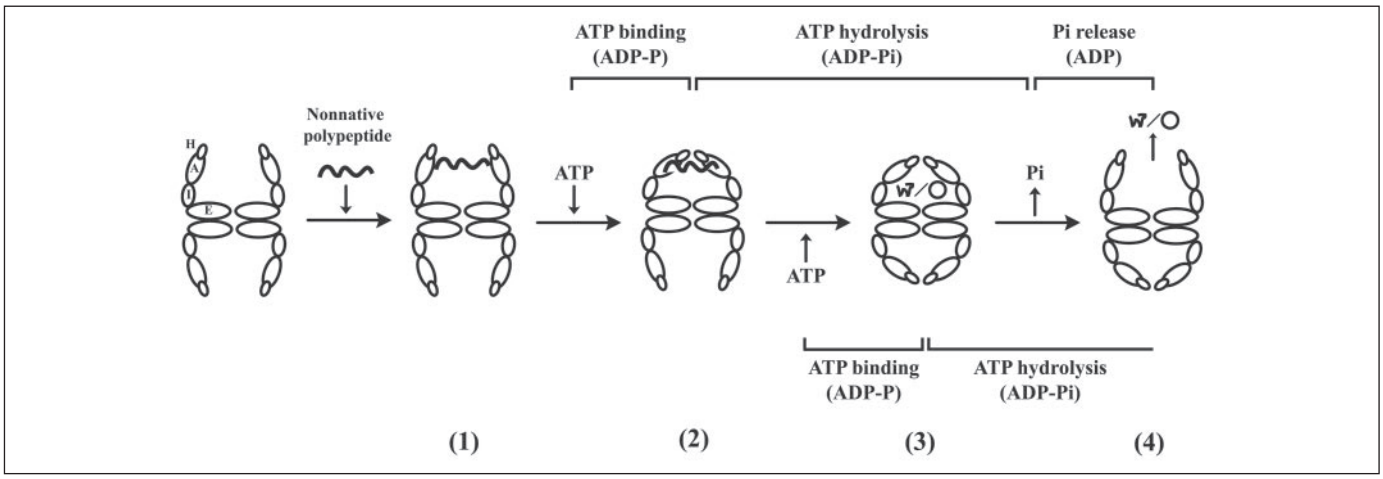

FIGURE 7. **Schematic model for the reaction mechanism of archaeal group II chaperonins.** See text for details. *A*, *I*, and *E* refer to the apical, intermediate, and equatorial domains, respectively. *H* represents the helical protrusion.

hydrolysis in the ring-bound substrate may be required for triggering the productive folding.

When the substitution of inorganic phosphate by metal fluoride is performed during ATP hydrolysis, both AlF_x and BeF_x induce α-chaperonin to adopt a football-like conformation, in which both rings are closed (Figs. 1–4). Nucleotide analyses have shown that αWT retained ADP and ATP (TABLE ONE). These results suggest that one ring is saturated with ADP and metal fluorides, and the other is filled with ATP. A detailed characterization of *T.* KS-1 chaperonins in the presence of ATP and BeF_x will be reported elsewhere.[3] Besides, we revealed that several phases exist in the conformational change induced by ATP binding in kinetic analyses.[4] From these results, it is thought that the symmetric closed conformation is also a transient intermediate in the functional cycle, and that it mediates the switch to alternate the active ring. Llorca *et al.* (16) reported that the binding of ATP to CCT generates an asymmetric particle; one ring is closed and the other has a slightly different conformation from the nucleotide-free form. It is likely that the binding of ATP to the other ring is promoted when one ring is filled with ATP in group II chaperonins.

The existing evidence indicates that asymmetric and symmetric molecules are found in the functional ATPase cycle of group II chaperonins. Based on these results, we propose a new model for the reaction mechanism of archaeal group II chaperonins (Fig. 7). In the absence of nucleotide, the chaperonin takes an open conformation and captures nonnative polypeptide (Fig. 7, *step 1*). Although the exact location of the substrate-binding site is not defined, it is likely that non-native substrates interact via the exposed hydrophobic surface of the apical domain. Subsequently, the binding of ATP leads to the conformational change to the asymmetric structure, in a similar manner to ATP and GroES binding with the substrate-bound ring of GroEL (Fig. 7, *step 2*). Contrary to the previous model, protein folding is not induced only by the closing of the lid, and further conformational change seems to be required. The asymmetric conformation changes to the symmetric closed conformation with the binding of ATP in the other ring. The substrate is released from the cavity wall into the hydrophilic central cavity where productive folding occurs (Fig. 7, *step 3*). Consequently, the release of the γ-phosphate generated by ATP hydrolysis in the folding-active ring triggers the opening of the lid and release of the substrate (Fig. 7, *step 4*). We speculate that the two rings of group II chaperonins alternate as a folding chamber in common with that of GroEL, and that the group II chaperonins have a similar molecular mechanism to GroEL and its partner GroES.

[3] T. Yoshida, R. Iizuka, K. Itami, T. Yasunaga, H. Sakuraba, T. Ohshima, M. Yohda, and T. Maruyama, manuscript in preparation.
[4] R. Iizuka, T. Inobe, K. Kuwajima, and M. Yohda, unpublished data.

REFERENCES

1. Bukau, B., and Horwich, A. L. (1998) *Cell* **92,** 351–366
2. Hartl, F. U., and Hayer-Hartl, M. (2002) *Science* **295,** 1852–1858
3. Gutsche, I., Essen, L. O., and Baumeister, W. (1999) *J. Mol. Biol.* **293,** 295–312
4. Conway de Macario, E., Maeder, D. L., and Macario, A. J. (2003) *Biochem. Biophys. Res. Commun.* **301,** 811–812
5. Klunker, D., Haas, B., Hirtreiter, A., Figueiredo, L., Naylor, D. J., Pfeifer, G., Muller, V., Deppenmeier, U., Gottschalk, G., Hartl, F. U., and Hayer-Hartl, M. (2003) *J. Biol. Chem.* **278,** 33256–33267
6. Lorimer, G. (1997) *Nature* **388,** 720–721
7. Rye, H. S., Burston, S. G., Fenton, W. A., Beechem, J. M., Xu, Z., Sigler, P. B., and Horwich, A. L. (1997) *Nature* **388,** 792–798
8. Rye, H. S., Roseman, A. M., Chen, S., Furtak, K., Fenton, W. A., Saibil, H. R., and Horwich, A. L. (1999) *Cell* **97,** 325–338
9. Ditzel, L., Lowe, J., Stock, D., Stetter, K. O., Huber, H., Huber, R., and Steinbacher, S. (1998) *Cell* **93,** 125–138
10. Gutsche, I., Holzinger, J., Rauh, N., Baumeister, W., and May, R. P. (2001) *J. Struct. Biol.* **135,** 139–146
11. Llorca, O., Martin-Benito, J., Grantham, J., Ritco-Vonsovici, M., Willison, K. R., Carrascosa, J. L., and Valpuesta, J. M. (2001) *EMBO J.* **20,** 4065–4075
12. Yoshida, T., Kawaguchi, R., Taguchi, H., Yoshida M., Yasunaga, T., Wakabayashi, T., Yohda, M., and Maruyama, T. (2002) *J. Mol. Biol.* **315,** 73–85
13. Meyer, A. S., Gillespie, J. R., Walther, D., Millet, I. S., Doniach, S., and Frydman, J. (2003) *Cell* **113,** 369–381
14. Iizuka, R., Yoshida, T., Shomura, Y., Miki, K., Maruyama, T., Odaka, M., and Yohda, M. (2003) *J. Biol. Chem.* **278,** 44959–44965
15. Iizuka, R., So, S., Inobe, T., Yoshida, T., Zako, T., Kuwajima, K., and Yohda, M. (2004) *J. Biol. Chem.* **279,** 18834–18839
16. Llorca, O., Smyth, M. G., Carrascosa, J. L., Willison, K. R., Radermacher, M., Steinbacher, S., and Valpuesta, J. M. (1999) *Nat. Struct. Biol.* **6,** 639–642
17. Yoshida, T., Yohda, M., Iida, T., Maruyama, T., Taguchi, H., Yazaki, K., Ohta, T., Odaka, M., Endo, I., and Kagawa, Y. (1997) *J. Mol. Biol.* **273,** 635–645
18. Yoshida, T., Yohda, M., Iida, T., Maruyama, T., Taguchi, H., Yazaki, K., Ohta, T., Odaka, M., Endo, I., and Kagawa, Y. (2000) *J. Mol. Biol.* **299,** 1399–1400
19. Bigay, J., Deterre, P., Pfister, C., and Chabre, M. (1987) *EMBO J.* **6,** 2907–2913
20. Fisher, A. J., Smith, C. A., Thoden, J. B., Smith, R., Sutoh, K., Holden, H. M., and Rayment, I. (1995) *Biochemistry* **34,** 8960–8972
21. Menz, R. I., Walker, J. E., and Leslie, A. (2001) *Cell* **106,** 331–341
22. Melki, R., and Cowan, N. J. (1994) *Mol. Cell. Biol.* **14,** 2895–2904
23. Melki, R., Batelier, G., Soulie, S., and Williams, R. C., Jr. (1997) *Biochemistry* **36,** 5817–5826
24. Inobe, T., Kikushima, K., Makio, T., Arai, M., and Kuwajima, K. (2003) *J. Mol. Biol.* **329,** 121–134
25. Chaudhry, C., Farr, G. W., Todd, M. J., Rye, H. S., Brunger, A. T., Adams, P. D., Horwich, A. L., and Sigler, P. B. (2003) *EMBO J.* **22,** 4877–4887

26. Taguchi, H., Tsukuda, K., Motojima, F., Koike-Takeshita, A., and Yoshida, M. (2004) *J. Biol. Chem.* **279,** 45737–45743
27. Sakikawa, C., Taguchi, H., Makino, Y., and Yoshida, M. (1999) *J. Biol. Chem.* **274,** 21251–21256
28. Iizuka, R., Yoshida, T., Maruyama, T., Shomura, Y., Miki, K., and Yohda, M. (2001) *Biochem. Biophys. Res. Commun.* **289,** 1118–1124
29. Motojima, F., and Yoshida, M. (2003) *J. Biol. Chem.* **278,** 26648–26654
30. Frank, J., Shimkin, B., and Dowse, H. (1981) *Ultramicroscopy* **6,** 343–358
31. Frank, J., Radermacher, M., Penczek, P., Zhu J., Li, Y., Ladjadj, M., and Leith, A. (1996) *J. Struct. Biol.* **116,** 190–199
32. Arai, M., Ito, K., Inobe, T., Nakao, M., Maki, K., Kamagata, K., Kihara, H., Amemiya, Y., and Kuwajima, K. (2002) *J. Mol. Biol.* **321,** 121–132
33. Arai, M., Inobe, T., Maki, K., Ikura, T., Kihara, H., Amemiya, Y., and Kuwajima, K. (2003) *Protein Sci.* **12,** 672–680
34. Semenyuk, A. V., and Svergun, D. I. (1991) *J. Appl. Crystallog.* **24,** 537–540
35. Bochkareva, E. S., Lissin, N. M., Flynn, G. C., Rothman, J. E., and Girshovich, A. S. (1992) *J. Biol. Chem.* **267,** 6796–6800
36. Murai, N., Makino, Y., and Yoshida, M. (1996) *J. Biol. Chem.* **271,** 28229–28234
37. Langer, T., Pfeifer, G., Martin, J., Baumeister, W., and Hartl, F. U. (1992) *EMBO J.* **11,** 4757–4765
38. Shomura, Y., Yoshida, T., Iizuka, R., Maruyama, T., Yohda, M., and Miki, K. (2004) *J. Mol. Biol.* **335,** 1265–1278
39. Gao, Y., Thomas, J. O., Chow, R. L., Lee, G. H., and Cowan, N. J. (1992) *Cell* **69,** 1043–1050
40. Martin, J., Langer, T., Boteva, R., Schramel, A., Horwich, A. L., and Hartl, F. U. (1991) *Nature* **352,** 36–42
41. Miyazaki, T., Yoshimi, T., Furutsu, Y., Hongo, K., Mizobata, T., Kanemori, M., and Kawata, Y. (2002) *J. Biol. Chem.* **277,** 50621–50628
42. Ueno, T., Taguchi, H., Tadakuma, H., Yoshida, M., and Funatsu, T. (2004) *Mol. Cell* **14,** 423–434